The Monte Carlo Method: Versatility Unbounded In A Dynamic Computing World
Chattanooga, Tennessee, April 17–21, 2005, on CD-ROM, American Nuclear Society, LaGrange Park, IL (2005)

DEVELOPMENT OF THE ADEIS VARIANCE REDUCTION METHODOLOGY FOR COUPLED ELECTRON-PHOTON TRANSPORT

Benoit Dionne[*] and Alireza Haghighat
Department of Nuclear and Radiological Engineering
University of Florida
202 Nuclear Science Center, P.O. Box 118300
Gainesville, FL, 32611
dionneb@ufl.edu; haghighat@ufl.edu

ABSTRACT

This paper presents a new variance reduction methodology, ADEIS (Angular-dependent adjoint Driven Electron-photon Importance Sampling), for coupled electron-photon Monte Carlo calculations. The methodology uses a modified version of the MCNP5 weight-window technique to perform transport biasing using angular-dependent lower-weight bounds. The lower-weight bounds are determined using deterministic importance functions calculated by the CEPXS/ONELD package. Note, similar to the CADIS methodology, the ADEIS formulation, currently derived for mono-energetic pencil beam, ensures the consistency between the source and the weight-window. ADEIS performance was examined for a homogeneous electron-only problem and a heterogeneous coupled electron-photon problem. Significant speedups (a few orders of magnitude) have been achieved for electron-only simulations, and electron tally estimation in coupled electron-photon simulations. Fluctuations were observed in the photon tallies, and remedies to remove these fluctuations were examined.

Key Words: Variance Reduction, Deterministic Importance, Electron-Photon

1 INTRODUCTION

Monte Carlo (MC) coupled electron-photon transport calculations are generally performed to determine various characteristics, such as energy or charge deposition, of systems exposed to radiation fields. However, tracking of all particles, primary and secondary, in complex geometry requires large amount of computational resources. Therefore, it is often useful to use variance reduction techniques to obtain results in a reasonable amount of time.

This paper presents the development of the ADEIS (Angular-dependent adjoint Driven Electron-photon Importance Sampling) variance reduction (VR) methodology for coupled electron-photon transport. This methodology uses deterministic importance functions to estimate angular lower-weight bounds for a modified version of the weight-window technique of MCNP5 [1]. The importance functions are calculated using the CEPXS/ONELD [2] package which performs one-dimensional coupled electron-photon transport calculation.

To analyze the performance of ADEIS, two one-dimensional problems are considered: an electron-only transport simulation in a homogeneous medium; and, a coupled electron-photon transport simulation in a heterogeneous medium. These problems are designed based on a *real-life* three-dimensional radiotherapy linear accelerator system.

[*] Corresponding author

This paper is organized in five sections. Section 2 presents the ADEIS methodology and some relevant background. Section 3 describes the test problems used for the electron-only and coupled electron-photon analyses. Section 4 presents the results and discussions for different analyses performed during the development of ADEIS. Finally, Section 5 summarizes the results and suggests future work.

2 ADEIS METHODOLOGY

The ADEIS (Angular-dependent adjoint Driven Electron-photon Importance Sampling) methodology is derived from the CADIS (Consistent Adjoint Driven Importance Sampling) methodology [3] which combines source and transport biasing within the MCNP weight-window technique [4]. This section presents brief overviews of the weight-window technique and the CADIS methodology, followed by a discussion on specific features of ADEIS.

2.1 Weight-Window Technique

The weight-window VR technique is a method where the particle population is controlled by playing Russian Roulette or particle splitting games to keep the particle statistical weights within a user-defined window. This implies that if a particle weight is below a lower-weight limit, the Russian Roulette game is played and if it survives the game, its weight is increased to a value within the window. On the contrary, if a particle weight is above an upper-weight limit, it is split so resulting weights are within the window. However, in this technique, the lower-weight bounds must be provided by the user for space-energy transparent meshes while upper-weight bounds are calculated using a user-specified multiple of the lower-weight bounds. It must be noted that the *transparent* mesh is independent of the problem geometry definition where the particle tracking is performed.

Note that for electrons, weights are checked against the weight-window after each energy step of the condensed-history (CH) algorithm. While, for photons weights are checked at least every mean free path.

2.2 CADIS Methodology

The CADIS methodology combines source biasing and transport biasing within the weight-window technique. The formulation for the biased source is given by

$$\hat{\mathbf{q}}(\vec{\mathbf{r}},\mathbf{E}) = \frac{\boldsymbol{\psi}^{+}(\vec{\mathbf{r}},\mathbf{E})\mathbf{q}(\vec{\mathbf{r}},\mathbf{E})}{\mathbf{R}}, \tag{1}$$

where $\mathbf{q}(\vec{\mathbf{r}},\mathbf{E})$ is the unbiased source, $\hat{\mathbf{q}}(\vec{\mathbf{r}},\mathbf{E})$ is the biased source and R is the response expressed by

$$\mathbf{R} = \int \mathbf{dEdV}\mathbf{q}(\vec{\mathbf{r}},\mathbf{E})\boldsymbol{\psi}^{+}(\vec{\mathbf{r}},\mathbf{E}). \tag{2}$$

Since the source variables are sampled from a biased probability density function, the statistical weight of the source particles must be corrected according to

$$\mathbf{w}(\vec{\mathbf{r}},\mathbf{E}) = \frac{\mathbf{R}}{\boldsymbol{\psi}^{+}(\vec{\mathbf{r}},\mathbf{E})}. \tag{3}$$

Note that the source biasing also maintains the consistency between the source and weight-window definitions.

For transport biasing, the number of particles that are transferred from one phase space to another is altered based on the ratio of the importance function and the splitting/rouletting games. In order to preserve the expected number of particles following this process, the particle statistical weights are modified according to

$$\mathbf{w}(\vec{\mathbf{r}},\mathbf{E}) = \mathbf{w}(\vec{\mathbf{r}}',\mathbf{E}')\left[\frac{\boldsymbol{\psi}^{+}(\vec{\mathbf{r}}',\mathbf{E}')}{\boldsymbol{\psi}^{+}(\vec{\mathbf{r}},\mathbf{E})}\right]. \tag{4}$$

Considering the MCNP weight-window implementation, the lower-weight bounds, as determined by the CADIS formulation for transport biasing, are given by

$$\mathbf{w}_{\mathbf{L}}(\vec{\mathbf{r}},\mathbf{E}) = \frac{\mathbf{R}}{\boldsymbol{\psi}^{+}(\vec{\mathbf{r}},\mathbf{E})\left(\frac{\mathbf{1}+\mathbf{c}}{\mathbf{2}}\right)}. \tag{5}$$

In Eq. 5, $\mathbf{w}_{\mathbf{L}}(\vec{\mathbf{r}},\mathbf{E})$ is the lower-weight bound, and **c** is a user defined parameter, which relates the upper-weight and lower-weight bounds as $\mathbf{w}_{\mathbf{U}}(\vec{\mathbf{r}},\mathbf{E}) = \mathbf{c}\,\mathbf{w}_{\mathbf{L}}(\vec{\mathbf{r}},\mathbf{E})$.

2.3 ADEIS Specific Features

Most of the problems of interest requiring electron-photon transport involve beam sources that are often considered mono-energetic. Therefore, at this point, the ADEIS methodology does not perform source biasing because the expected gain for such problems is minimal (even zero in the case of a mono-energetic pencil beam). Note that the consistency between the source and the weight-window is achieved without source biasing as described later. ADEIS automates the generation of weight-window lower-weight bounds and various other parameters by generating the standard MCNP5 interface file *wwinp*. However, the generation of the deterministic model is not automated. Fig. 1 shows the different steps involved in an ADEIS calculation.

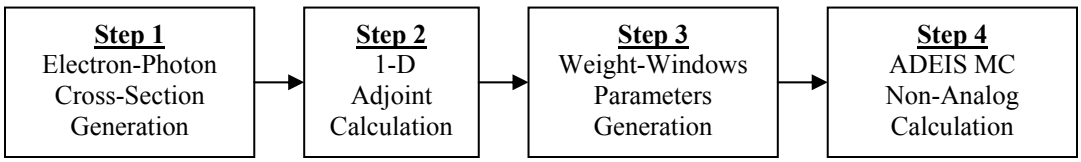

Figure 1 Four steps of ADEIS

Each of these steps is discussed in more details in the following four subsections.

2.3.1 Lower-weight bounds determination

ADEIS calculates the lower-weight bounds of the weight-window in a slightly different way then CADIS. The lower-weights bound are calculated according to the following formulation

$$\mathbf{w_L(\vec{r},E) = \frac{R}{\psi^+(\vec{r},E)\,c}} \tag{6}$$

Here, the source particles are generated at the upper-weight bounds of the weight-window, resulting in a consistent formulation without source biasing for the problem of interest. This can be demonstrated by deriving the lower-weight and upper-weight bounds at the surface ($\vec{\mathbf{r}}_0$). This formulation has two main advantages. First, when mono-energetic surface sources are used, there is no need to adjust the weights of the source particles to be within the window as is demonstrated by the following discussions. For a mono-energetic point source, the response R is given by

$$\mathbf{R = \int dEdVq(\vec{r},E)\psi^+(\vec{r},E) = \int dEdV\,\delta(\vec{r}-\vec{r}_0)\,\delta(E-E_0)\,\psi^+(\vec{r},E) = \psi^+(\vec{r}_0,E_0)} \tag{7}$$

where $\delta(\vec{\mathbf{r}}-\vec{\mathbf{r}}_0)$ and $\delta(\mathbf{E}-\mathbf{E}_0)$ are the Dirac delta function representing a unit surface mono-energetic ($\mathbf{E}_0$) source. Using Eq. 7 we can rewrite the lower-weight and upper-weight at the surface as follows

$$\mathbf{w_L(\vec{r}_0,E_0) = \frac{R}{\psi^+(\vec{r}_0,E_0)\,c} = \frac{\psi^+(\vec{r}_0,E_0)}{\psi^+(\vec{r}_0,E_0)\,c} = \frac{1}{c}} \tag{8}$$

$$\mathbf{w_U(\vec{r}_0,E_0) = c\,w_L(\vec{r}_0,E_0) = 1} \tag{9}$$

In this way, consistency between the source and the weight-window is achieved. The second advantage is that by "starting" the source particle at the upper-weight bound of the weight-window, an additional increase in speedup is obtained.

Due to the numerical difficulties inherent in the deterministic electron-photon transport calculations, the importance functions exhibit unphysical oscillations. Mainly, CEPXS/ONELD methodology produces negative importance functions which cannot be used to calculate physical quantities such as the lower-weight bounds. ADEIS eliminates these unphysical oscillations by a simple averaging procedure. Previous studies [5] using the CADIS methodology showed that such approximated importance functions still increased the figure-of-merit (FOM) significantly.

2.3.2 Importance function calculation using CEPXS/ONELD

To generate the required importance functions (see Eq. 6), ADEIS utilizes the publicly available CEPXS/ONELD package. Note that the package's preprocessing codes cannot be used for adjoint calculations; therefore, a set of processing codes were developed.

ONELD calculates the importance associated with each phase-space mesh by using the one-dimensional adjoint linear Boltzmann equation (ALBE), Eq. 10, which is solved using the S_N method.

$$-\mu\frac{\partial}{\partial x}\psi^{+}(x,E,\mu)+\sigma_{t}(x,E)\,\psi^{+}(x,E,\mu)= \\ +\int_{4\pi}d\Omega'\int_{0}^{\infty}dE'\sigma_{s}(x,E\rightarrow E',\mu_{0})\,\psi^{+}(\vec{r},E',\mu')+S^{+}(x,E,\mu) \tag{10}$$

For electrons, however, the use of the ALBE with the standard Legendre expansion of the scattering kernel is impractical because of the need to use an unreasonably high expansion order. This would be necessary because of the highly anisotropic behavior of the electron scattering process. In order to improve the efficiency of the electron transport calculation, CEPXS generates *effective* cross sections by using the following treatments:

i) A continuous slowing-down (CSD) [6] approximation is used for electron inelastic scattering interactions resulting in small-energy changes (often referred to as soft collisions).

ii) The extended transport correction [7] is applied to the forward-peaked elastic scattering cross-section.

Note that by using these cross sections in ONELD, this approach effectively solves the Boltzmann-CSD equation, which is better suited for electron transport.

2.3.3 Angular biasing

Since most problems of interest utilize electron beam sources, and electrons are scattered mainly in the "forward" direction (as well as the generated photons), the resultant flux distributions are highly angular dependent. Therefore, to achieve a higher efficiency, it is expected that the bounds of the weight-window should be angular dependent also. To address this issue in the context of an adjoint-based VR, we calculate the angular lower-weight bounds based on the following formulations,

$$w_{L,\pm}(\vec{r},E)=\frac{R}{\varphi_{\pm}^{+}(\vec{r},E)\,c}, \tag{11}$$

where,

$$\varphi_{\pm}^{+}(\vec{r},E)=\int_{\substack{+:\mu>0\\-:\mu<0}}d\mu\;\psi^{+}(\vec{r},E,\mu). \tag{12}$$

Note that the use of above formulations requires the modification of the standard MCNP5 weight-window algorithm.

3 TEST PROBLEM DESCRIPTIONS

To examine the performance of ADEIS, two test problems are considered. One problem simulates electron-only transport in a homogeneous medium, and the other problem simulates coupled electron-photon transport in a heterogeneous medium.

3.1 Electron-Only Problem

For the electron-only problem, a mono-directional 13 MeV electron beam, impinging on the left-hand side of a water phantom, is considered (see Fig. 1). The shaded volume represents the tallying region, which is located just beyond the range of the 13 MeV electrons (between 6.35 cm and 6.5 cm).

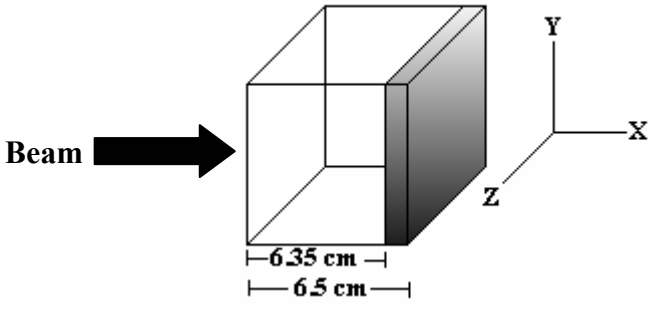

Figure 1 Homogeneous Water Phantom

Table II gives the main simulation parameters for both the MC and adjoint deterministic calculations.

Table I. Electron-only Simulation Parameters

Monte Carlo	Electron-only Adjoint Transport
Electrons only	50 energy groups
Energy straggling is not sampled	S_{16}-P_{15}
Cutoff at 0.01 MeV	Flat adjoint source spectrum
Default value for ESTEP in CH algorithm	85 spatial meshes

Note that for this study, the energy straggling is not sampled because the CEPXS/ONELD package does not account for the soft collision. This leads to an importance function distribution that does not correspond to the physical processes being simulated in the MC calculation. Consequently, this shortcoming may yield biased results, so, in this exercise, the sampling of the energy straggling distribution is deactivated in MCNP5. Note that the deterministic simulation parameters are based on recommendations given in the CEPXS/ONELD user's guide [2] for the *forward* calculations.

3.2 Coupled Electron-Photon Problem

For the coupled electron-photon problem, a mono-energetic 6 MeV electron beam is impinging on a tungsten target producing bremsstrahlung photons, which are transported through a heterogeneous geometry (representing an accelerator head) shown in Fig. 2.

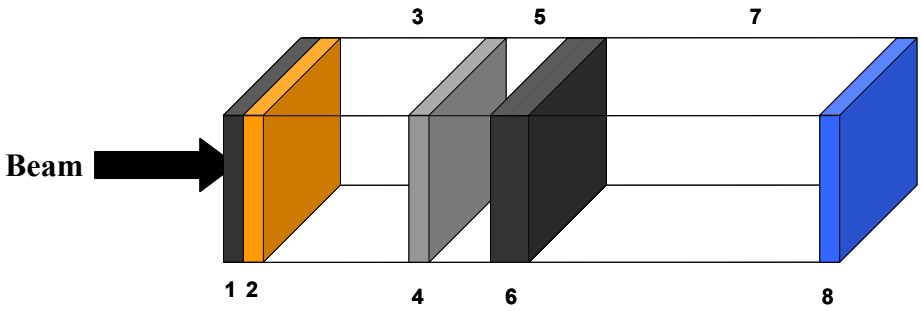

Figure 2 Simplified 1-D Accelerator Head

The region of interest (ROI), colored in blue, is a layer of water located at 100 cm away from the source. Note that this figure is not to scale. The details associated with each zone of Fig. 2 are presented in Table II.

Table II. Geometry Description

Zone	Description	Color	Material	Size (cm)
1	Target	Dark Gray	Tungsten	0.1
2	Heat Dissipator	Orange	Copper	0.15
3	Vacuum	White	Low Density Air	8.75
4	Vacuum Window	Light Gray	Beryllium	0.05
5	Air	White	Air	1.1
6	Flattening Filter	Dark Gray	Tungsten	1.0
7	Air	White	Air	88.85
8	Region of Interest	Blue	Water	0.1

The main parameters for both MC and adjoint deterministic coupled electron-photon simulations are presented in Table III.

Table III. Electron-Photon Simulation Parameters

Monte Carlo	Electron-Photon Adjoint Transport
Electrons and photons	50 electron groups 30 photon groups
Energy straggling is not sampled	S_{16}-P_{15}
Cutoff at 0.01 MeV	Flat adjoint source spectrum
Default value for ESTEP in CH algorithm	135 spatial meshes

4 RESULTS & ANALYSES

This section presents analyses for electron-only and coupled electron-photon simulations. Subsections 4.1 to 4.3 are dedicated to the results obtained from electron-only calculations, while

Subsections 4.4 and 4.5 are dedicated to the results obtained from the coupled electron-photon simulations.

4.1 Electron-only Problem

4.1.1 Efficiency trends without angular biasing

For a given problem, it is expected that the effectiveness of the ADEIS methodology is related to the probability of transmission of the source particles to the ROI. To demonstrate this, the ROI is move closer and closer to the source, therefore, increasing the probability of transmission. Fig. 3 illustrates the location of the region of interest for the test cases (at 5.5 cm, 6.0 cm, 6.2 cm and 6.35 cm) considered.

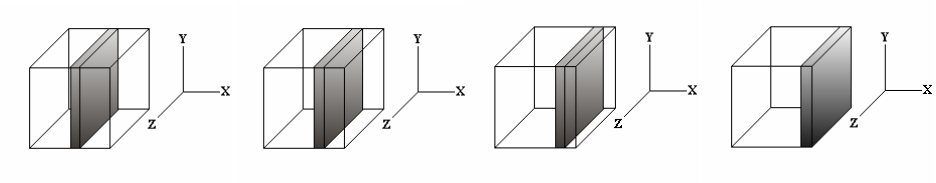

Figure 3 Region of Interest Location

For each of these cases, the speedup is estimated by

$$\mathbf{Speedup} = \frac{\mathbf{FOM}_{\mathbf{non-analog}}}{\mathbf{FOM}_{\mathbf{analog}}}, \tag{13}$$

and the probability of transmission (POT) is determined by

$$\mathbf{POT} = \frac{\mathbf{Number\ of\ particles\ entering\ the\ ROI}}{\mathbf{Total\ number\ of\ source\ particles}}. \tag{14}$$

Fig. 4 shows the speedup as a function of the probability of transmission.

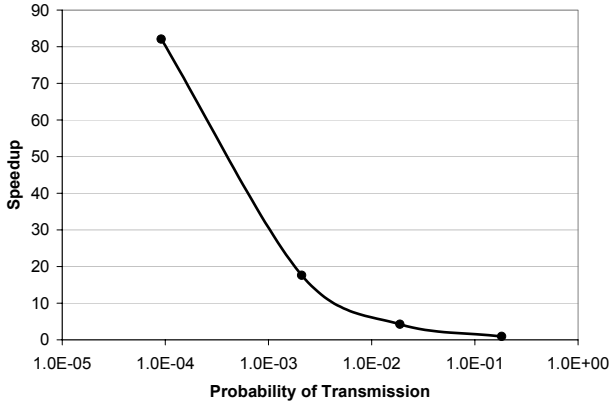

Figure 4 Speedup as a Function of Probability of Transmission

As expected, the methodology becomes more effective as the probability of transmission decreases.

4.1.2 Analog and non-analog electron tracks

It is useful to look at the electron tracks within the water phantom in order to understand the impact of the ADEIS VR technique, which *selects* the particles having a better chance of reaching the ROI. Fig. 5 shows the analog and non-analog electron tracks for the test problem. Note that only 1000 histories were simulated to generate these figures.

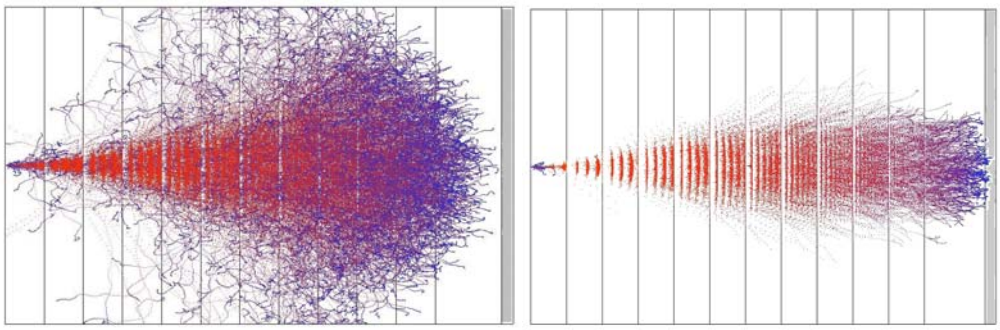

Figure 5 Electron Tracks in Water Phantom (left: analog; right: non-analog)

The colors represent the energy of the electrons, red being the highest and blue the lowest. By comparing the figures, it is obvious that electrons having a low probability of contribution to the ROI (shaded volume) are not followed, thereby resulting in an increasing FOM.

4.1.3 Impact of angular biasing

The impact of angular biasing is evaluated by comparing the performance of ADEIS with and without the use of angular-dependent lower weight bounds. Table IV presents the speedups for the test problem (Fig. 1) with and without angular biasing.

Table IV. Speedup with and without Angular Biasing

Case	Speedup
Without angular biasing	8.05
With angular biasing	28.98

It is obvious that angular biasing has a significant impact on the performance of ADEIS for this class of problem.

4.2 Coupled Electron-Photon Problem

This section presents the results obtained by tallying both the electron and photon scalar fluxes in the ROI (see Fig. 2) for the coupled electron-photon problem described in section 3.2.

4.2.1 Electron scalar flux tally

It is important to understand that the results presented in this section differ significantly than those presented in Section 4.1 to 4.3. These electrons are mainly secondary particles that are coupled to both the source electrons and the secondary photons. Fig. 7 shows the changes in the relative error and the FOM as a function of histories.

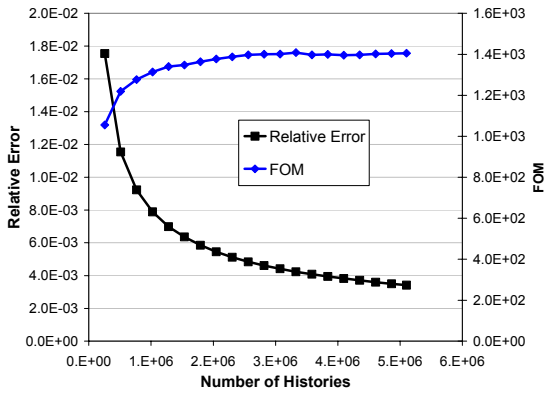

Figure 7 Electron Tally Relative Error and FOM

Fig.7 shows that the electron tally relative error and FOM behave as expected. To verify that no bias is introduced by the methodology, in Table V, we compare the analog and non-analog tallies and their associated relative error and FOM.

Table V. Electron Tally Results

Case	Mean	FOM
Analog	1.57E-06 (3.42%)*	13.65
Non-Analog	1.54E-06 (0.03%)	1404.5

*1-σ relative statistical uncertainty

Table V. shows that the analog and non-analog results agree within their statistical uncertainties, and the non-analog calculation shows a speedup of 103.

4.2.2 Photon scalar flux tally fluctuations

Due to the nature of the problem, there are significant differences in the importance functions of electrons and photons throughout model; therefore, large fluctuations can occur in the particle tallies. Fig. 8 shows the impact of these fluctuations on the relative error and FOM corresponding to the photon tally at the ROI.

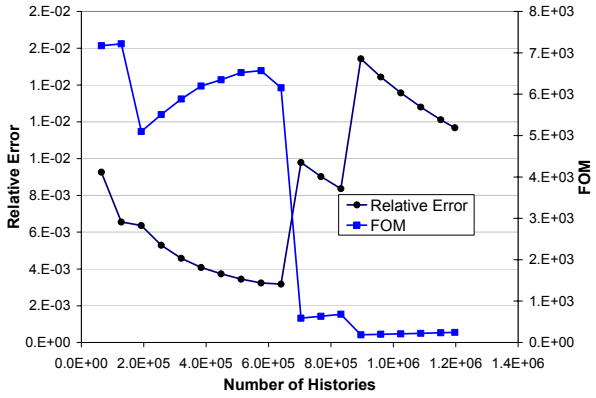

Figure 8 Fluctuation of the Photon Tally as a Function of Histories

To understand how the difference in importance functions may produce tally fluctuations, it is useful to examine one specific history. This history was selected based on the fact that it resulted in tally fluctuation caused by the particle's large weight. For example, a bremsstrahlung photon produced in the tungsten target (see Fig. 2 & Table II) may interact in the flattening filter (also made of tungsten) and produce an electron-positron pair. The positron may survive the Russian roulette and its weight may increase significantly due to the low importance of positrons in that region, as shown in Fig. 9. The low energy positron is rapidly

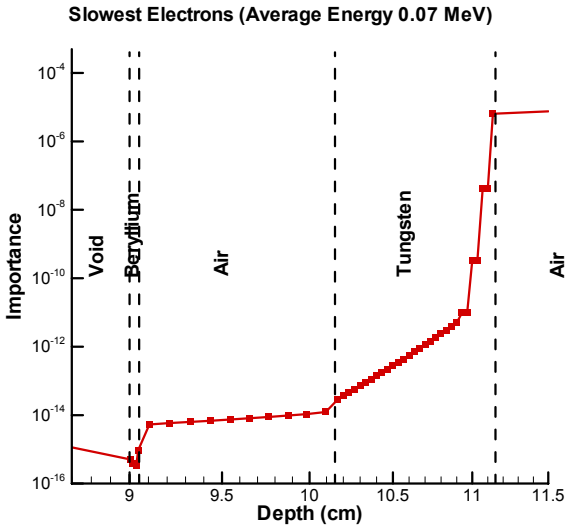

Figure 9 Electron Importance in the Flattening Filter

annihilated and the generated high weight photons reach the air region. These photons have a weight much higher than the upper limit of their weight-window, and therefore need to be splitted considerably to be brought back into the window. However, since the mean-free-path of the annihilation photon in air is large and the maximum splitting ratio is small (compared to the ratio of electron and photon importances at the tungsten-air interface, see Table VI), the splitting process cannot bring the weight within the bounds of the weight-window before photons reach the tally. Consequently, these high weight photons introduce fluctuations in the tally as shown in Fig. 8.

Table VI. Electron and Photon Importance at Air-Tungsten Interface

Electron Importance	1.58E-05
Photon Importance	2.27E-02
Importance Ratio	1440
Maximum Splitting Ratio	5

Besides sampling a large number of those high-weight particles (i.e., longer simulation time), we investigated two remedies to overcome this difficulty. These remedies are:

1. Modify the number of spatial meshes to better resolve the discontinuities in the importance function distribution.

2. Do not bias the electrons within regions where the importance changes too drastically.

Note that in order to properly study this issue, the angular biasing was deactivated.

Number of transparent meshes

Since the problem is due to the discontinuity in the importances, in the region close to the air-tungsten interface, the meshes are refined in an attempt to alleviate the tally fluctuations. Fig. 10 shows the variations in the FOM (due to the fluctuations in the tally) as a function of histories for the following mesh structures:

1. Mesh structure #1: increased the number of meshes in air by 50%.
2. Mesh structure #2: increased the number of meshes in the flattening filter by 66%, while decreasing the number of meshes in the copper target by the same percentage.
3. Mesh structure #3: increased the number of meshes in the flattening filter by 66%, and decreased the size of meshes in the first 20 cm of air by a factor of 4.
4. Mesh structure #4: increased the size of meshes by 1/4 in the first 0.85 cm of the flattening filter, but decreased the mesh size by a factor of 5 in the last 0.15 cm.

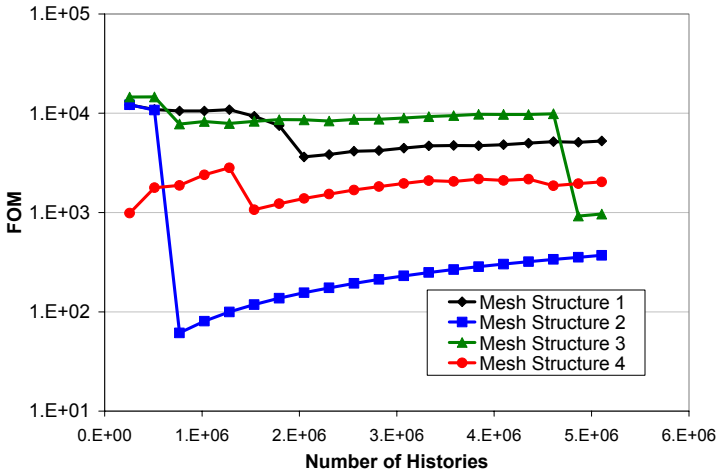

Figure 10 FOM as a Function of Histories

Fig. 10 indicates that the tally fluctuations cannot be completely eliminated by changing the mesh structure, but it still has a significant impact. In order to evaluate the *quality* of these simulations, we introduce the following formulation

$$(\mathbf{R}_{\mathbf{FOM}} = \frac{\mathbf{S}_{\mathbf{FOM}}}{\bar{\mathbf{x}}_{\mathbf{FOM}}}), \tag{14}$$

where $\mathbf{S}_{\mathbf{FOM}}$ is the standard deviation of the FOM estimated as a function of the histories, and $\bar{\mathbf{x}}_{\mathbf{FOM}}$ is the average of the FOM.

Table VII presents R_{FOM} for the different mesh structures.

Table VII. Relative Variation in FOM for 4 Mesh Structure

Mesh structure #1	0.44
Mesh structure #2	2.58
Mesh structure #3	0.37
Mesh structure #4	0.24

Based on this metric, the mesh structure #4 provides the best importance distribution, thereby, the lowest level of fluctuations. These results suggest that the quality of the importance plays a major role in coupled electron-photon simulation, and therefore, further investigation is needed.

No biasing in the flattening filter

In order to mitigate the tally fluctuations, we also considered not biasing regions in which the change of importance is too large. In this work, the region containing tungsten (i.e., flattening filter) exhibited this behavior. To deactivate the biasing within the most problematic part of the tungsten, the lower-weight bounds was set to zero between 11 cm and 11.15 cm (see Fig. 8) for the slowest electron energy group. Not considering biasing in this region, effectively removed the tally fluctuations, while resulting in significant reduction in FOM, from ~2000 to ~350. This FOM, however, is about half the analog FOM; therefore this remedy is not an effective approach.

5 CONCLUSIONS AND FUTURE WORK

We have presented a new variance reduction methodology, ADEIS (Angular-dependent adjoint Driven Electron-photon Importance Sampling), for coupled electron-photon Monte Carlo calculations.

The methodology uses a modified version of the MCNP5 weight-window technique to perform transport biasing using angular-dependent lower-weight bounds. The lower-weight bounds are determined using deterministic importance functions calculated by the CEPXS/ONELD package. Note, similar to the CADIS methodology, the ADEIS formulation, currently derived for mono-energetic pencil beam, ensures the consistency between the source and the weight-window.

ADEIS performance was examined for a homogeneous electron-only problem and a heterogeneous coupled electron-photon problem.

For the electron-only problem, it was observed that the speedup increases in range of 4 to 82 as the probability of transmission to the region of interest decreases (from .1 to 10-5). We also observed that this speedup can be increased by a factor of ~4 when the angular-dependent lower-weight bounds are used.

For the coupled electron-photon problem, we showed that the electron tally is well behaved and that speedup of about ~100 is possible. However, it was observed that the photon tally exhibited fluctuations due to the presence of significant discontinuities in the importances and the coupling between photons and electrons. It was shown that the fluctuations can be eliminated by not biasing the electron around the importance discontinuities. However, this approach resulted in a significant degradation of the figure-of-merit. We also showed that changing the

resolution of the spatial meshing to better resolve the discontinuities can mitigate fluctuations, but further investigations are needed.

For future work, we are considering several investigations including accounting for energy straggling for soft-collision, developing a robust algorithm dealing with the tally fluctuations, determination of coupled electron-photon deterministic adjoint in 3-D geometries for ADEIS, and perform parametric study for improving the efficiency of ADEIS.

6 REFERENCES

1. X-5 Monte Carlo Team, MCNP-A General Monte Carlo N-Particle Transport Code, Version 5 Volume II: User's Guide, Los Alamos National Laboratory, Report LA-CP-03-0245 (2003).

2.Lorence, L. J., Morel, J. E. and Valdez, G. D., User's Guide to CEPXS/ONELD: A One-Dimensional Coupled Electron-Photon Discrete Ordinates Code Package Version 1.0, Sandia National Laboratories, Report SAND89-1161 (1989).

3.Haghighat, A. and Wagner, J. C., "Monte Carlo Variance Reduction with Deterministic Importance Functions", *Progress of Nuclear Energy Journal*, **Vol. 42**, 1 (2003).

4.Briesmeister, J. F., Editor, MCNP – A General Monte Carlo Code N-Particle Transport Code, Version 4A, Los Alamos National Laboratory, Report LA-12625 (1993).

5.Wagner J.C., Acceleration of Monte Carlo Shielding Calculations with an Automated Variance Reduction Technique and Parallel Processing, Ph.D. Thesis, The Pennsylvania State University, Nuclear Engineering Dept. (1997).

6.Morel, J. E., "Fokker-Planck Calculations Using Standard Discrete Ordinates Transport Codes", Nuclear Science and Engineering, 79, 340-356 (1981).

7.Morel, J. E., "On the Validity of the Extended Transport Cross-Section Correction for Low-Energy Electron Transport", Nuclear Science and Engineering, 71, 64-71 (1979).